Supporting Information

Mg-doping improves the performance of Ru-based electrocatalyst for acidic oxygen evolution reaction

Zheng Li,[ab] Shuo Wang,[b] Yuanyuan Tian,[b] Baihai Li,[d] Hao jun Yan,[e] Shuai Zhang,[e] Zhaoming Liu,[*a] Qiuju Zhang,[*bc] Yichao Lin[*bc] and Liang Chen[bc]

a School of Materials Science and Engineering, Dalian Jiaotong University, Dalian 116028, P.R. China.
b Ningbo Institute of Materials Technology and Engineering, Chinese Academy of Sciences, Ningbo, Zhejiang 315201, P.R.China.
c University of Chinese Academy of Sciences, Beijing, 100049, P. R. China.
d School of Materials and Energy, University of Electronic Science and Technology of China, Chengdu 611731, Sichuan, China.
e Ningbo Electric Power Design Institute, Ningbo, Zhejiang 315000, China.

*Corresponding authors:

E-mail addresses: lzm100@163.com (Zhaoming Liu), zhangqj@nimte.ac.cn (Qiuju Zhang), yclin@nimte.ac.cn(Yichao Lin).

Experimental Section

Materials: All reagents are of analytical grade and used without purification. $Mg(NO_3)_2 \cdot 6H_2O$, Ruthenium chloride hydrate ($RuCl_3 \cdot xH_2O$), Polyvinylpyrrolidone K-30 ($(C_6H_9NO)_6$, PVP), DMF, ethyl alcohol (C_2H_5OH) and methyl alcohol (CH_3OH) were purchased from Sinopharm Chemical Reagent limited corporation. 2,5-Dihydroxyterephthalic acid were purchased from damas-beta. The commercial Ruthenium oxide (RuO_2) catalysts which is 99.9% (metals basis) pure anhydrous ruthenium oxide bought from Alfa Aesar are composed.

Characterization: The powder X-ray diffraction patterns of the samples were analysed with an X-ray diffractometer (German Bruker D8 Advance Davinci) using Cu-Kα radiation (λ=1.54178 Å) with 2θ range of 5-80. The morphology, size and energy dispersive X-ray (EDX) spectroscopy of all as-synthesized samples were characterized by a Talos F200x field-emission scanning electron microscopy. XPS was measured on an AXIS ULTRA X-ray photoelectron spectrometer using Mg Kα radiation. Using the BET (Brunauer-Emmet-Teller) and BJH (Barrett-Joyner-Halenda) methods to get the specific surface and pore diameters were obtained from the results of N_2 physisorption at 77 K (Micromeritics ASAP 2020) The inductively coupled plasma mass spectrometer (ICP-MS) (Perkin-Elmer, NexION 300X) is used to obtaine the content of Mg and Ru.

Experimental section

The chemicals were of analytical grade and used as received without further purification in this study.

Mg-MOF-74 synthesis. The Mg-MOF-74 was synthesized according to the literature reported[1]. $Mg(NO_3)_2 \cdot 6H_2O$ (0.2 mmol), 2,5-Dihydroxyterephthalic acid (0.1 mol) and poly vinylpyrrolidone were dispersed in a mixture of 6 mL DMF and 0.5 mL H_2O under stirring for 10 min, and then synthetic solution was transferred into a 50 ml Teflon-lined-stainless steel autoclave and kept at 393 K for 8 h. The autoclave was left to cool to room temperature. The resulting yellow product was obtained by centrifuge and washed with DMF and ethanol for three times to remove unreacted species from the framework. Finally, the yellow product was dried at 80 ^oC in air and collected for future use.[2]

Mg-RuO_2 synthesis.

The as-prepared Mg-MOF-74 (0.1 g) and $RuCl_3 \cdot xH_2O$ (0.1 g) were dispersed in 7.5 mL distilled water, and kept under agitated stirring in dark for 14 h. The resulting MOF derivate were collected and washed with distilled water for three times, then dried in an over at 80 ^oC. 100 mg of Mg-MOF-74 derivative precursor was heated at 300 to 400 °C for 4 h in the air atmosphere to produce Mg-RuO_2

nanocrystals.

Calculation details:

Spin-polarized density functional theory (DFT)[3] is performed in the Vienna ab initio simulation package (VASP).[4] The projected augmented-wave method (PAW)[5] potentials are adopted, together with the exchange–correlation energy of the general gradient approximation (GGA) in the scheme proposed by Perdew–Burke–Ernzerh (PBE).[6] The plane waves of the cut-off kinetic energies are set to 500 eV for all the calculations. In the process of structure relaxation the convergence tolerance of energy and force on each atom are less than 10^{-4} eV and 0.02 eV $Å^{-1}$. In bulk RuO_2 and RuO_2(110) surface, using a set of Monkhorst–Pack mesh K points of 3 × 3 × 5 to sample the Brillouin zone. To avoid the interactions between the two periods, the surface of the c axis is set to 15 Å to ensure sufficient vacuum. Dispersion correction is considered in the DFT-D_3 method to accurately describe the long-range van der Waals (vdW) interactions.[7, 8]

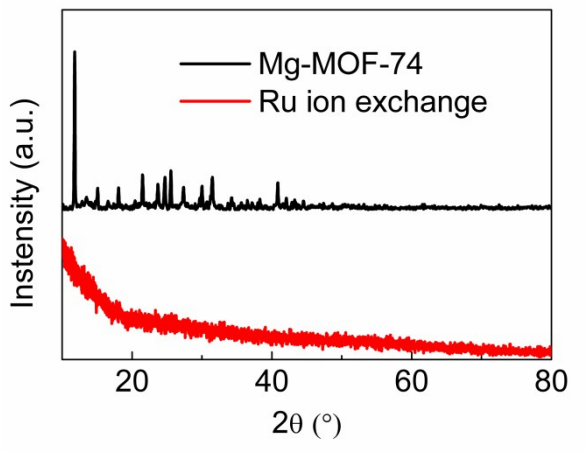

Fig. S1 the XRD of Mg-MOF-74 and Ru ion exchange

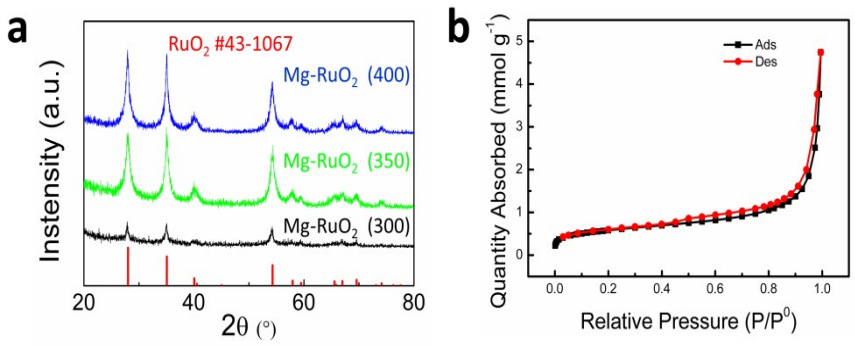

Fig. S2 a) The XRD comparison of RuO_2, Mg-RuO_2 (300), Mg-RuO_2 (350) and Mg-RuO_2 (400) to illustrate the crystal structure of Mg-RuO_2. b) The BET analysis of Mg-RuO_2 (350).

Table S1. Comparison of the OER electrocatalytic performances of RuO_2 in our work with those reported in literatures.

Catalyst	Current density	Electrolyte	Tafel slope	Overpotential at 10 mA cm^{-2} (mV)
RuO_2	10 mA cm^{-2}	0.5 M H_2SO_4	63.32 mV dec^{-1}	308[This work]
RuO_2	10 mA cm^{-2}	0.5 M H_2SO_4	64.47 mV dec^{-1}	298[9]
RuO_2	10 mA cm^{-2}	0.5 M H_2SO_4	-	289[10]
RuO_2	10 mA cm^{-2}	0.5 M H_2SO_4	179 mV dec^{-1}	312[11]
RuO_2	10 mA cm^{-2}	0.5 M H_2SO_4	64 mV dec^{-1}	297[12]
RuO_2	10 mA cm^{-2}	0.1 M $HClO_4$	-	430[13]
RuO_2	10 mA cm^{-2}	0.1 M $HClO_4$	73 mV dec^{-1}	332[14]

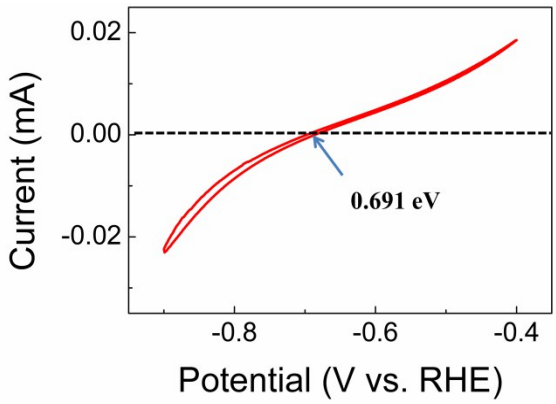

Fig. S3 The Hg/Hg_2SO_4 reference electrode was calibrated in H_2-saturated 0.5 M H_2SO_4 solution by measuring hydrogen oxidation/evolution at a platinum wire electrode and defining the point of zero current as 0 V versus reversible hydrogen electrode (RHE).

Table S2. Comparison of OER activities of Ru-based and Ir-based electrocatalysts in acidic media.

Catalyst	Current density	Electrolyte	Overpotential at 10 mA cm^{-2} (mV)
Mg-RuO_2	10 mA cm^{-2}	0.5 M H_2SO_4	228[This work]
$Cr_{0.6}Ru_{0.4}O_2$	10 mA cm^{-2}	0.5 M H_2SO_4	178[12]
Cu-doped RuO_2	10 mA cm^{-2}	0.5 M H_2SO_4	188[9]
Ru@IrO_x	10 mA cm^{-2}	0.05 M H_2SO_4	282[15]
RuCo@NC	10 mA cm^{-2}	0.5 M H_2SO_4	247[11]
Co-RuIr	10 mA cm^{-2}	0.1 M $HClO_4$	235[16]
PdO@RuO_2	10 mA cm^{-2}	0.1 M $HClO_4$	257[14]
$Y_{1.85}Zn_{0.15}Ru_2O_{7-\delta}$	10 mA cm^{-2}	0.5 M H_2SO_4	291[17]
$Y_2[Ru_{1.6}Y_{0.4}]O_{7-\delta}$	18.1 mA cm^{-2}	0.1 M $HClO_4$	270[18]
$Y_2Ru_2O_{7-\delta}$	1 mA cm^{-2}	0.1 M $HClO_4$	270[19]
Ir	10 mA cm^{-2}	0.5 M H_2SO_4	290[20]
$IrO_x/SrIrO_3$	10 mA cm^{-2}	0.5 M H_2SO_4	290[21]
Ir-STO	43 mA cm^{-2}	0.1 M $HClO_4$	295[22]
Ir_6Ag_9NTs	10 mA cm^{-2}	0.5 M H_2SO_4	285[23]
P-$IrCu_{1.4}$NCs	10 mA cm^{-2}	0.05 M H_2SO_4	311[24]
IrNi NCs	10 mA cm^{-2}	0.5 M H_2SO_4	280[25]
$W_{0.57}Ir_{0.43}O_{3-\delta}$	10 mA cm^{-2}	1 M H_2SO_4	370[26]
IrO_x-Ir	10 mA cm^{-2}	0.5 M H_2SO_4	290[27]

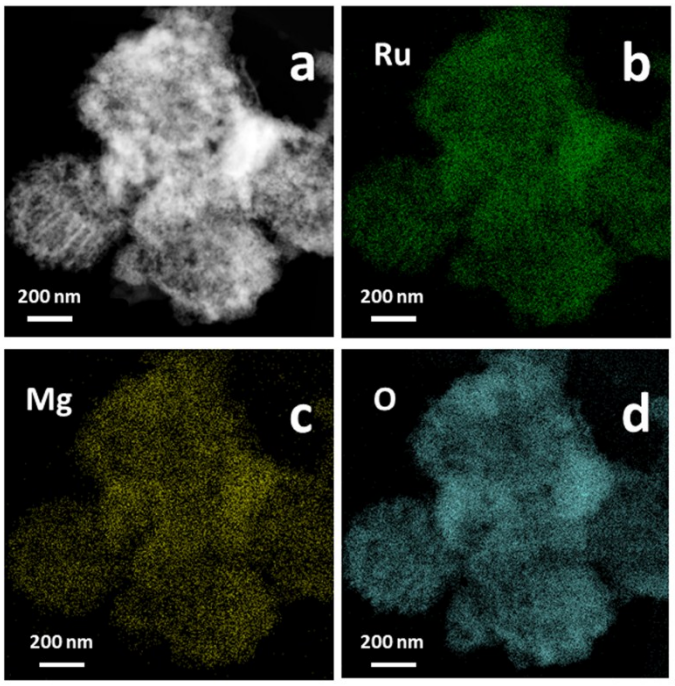

Fig. S4 a) the HAADF-STEM of Mg-RuO_2 (350) b-d) the EDX of Mg-RuO_2 (350) after 10,000 cycles for Ru(b),Mg(c) and O(d)

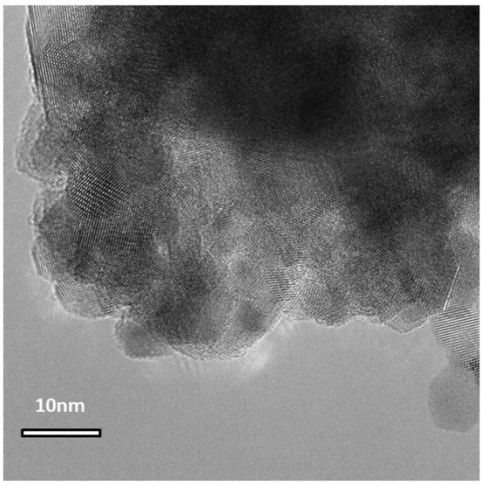

Fig. S5 the HRTEM image of Mg-RuO_2 (350) after 10, 000 CV cycles

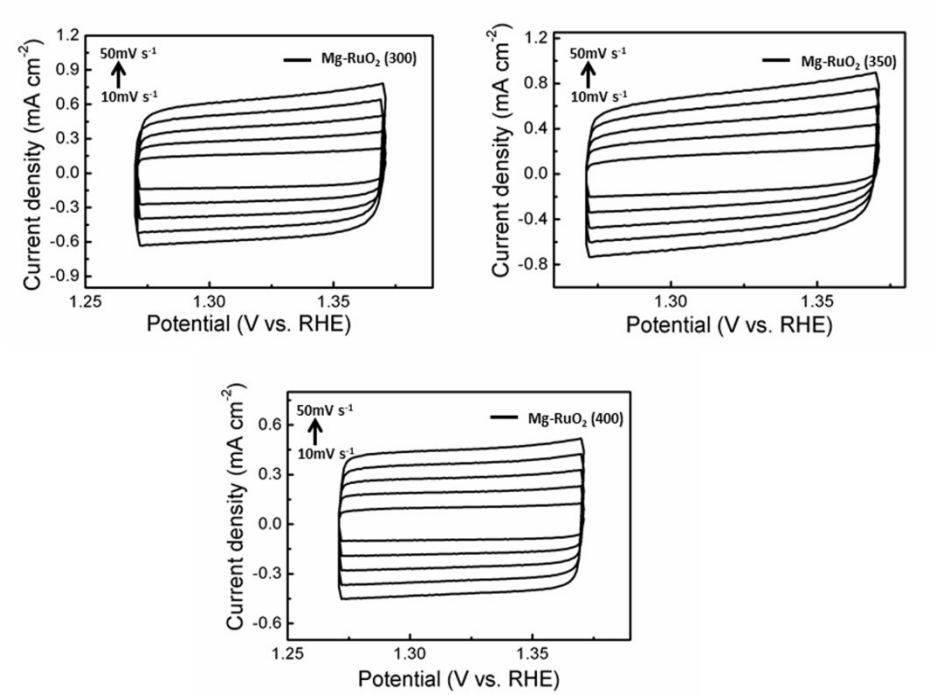

Fig. S6 CV curves measured within the range of 1.27 to 1.39 V vs. RHE with scan rate from 10 to 50 mV s^{-1} of Mg-RuO_2 (300), Mg-RuO_2 (350) and Mg-RuO_2 (400)

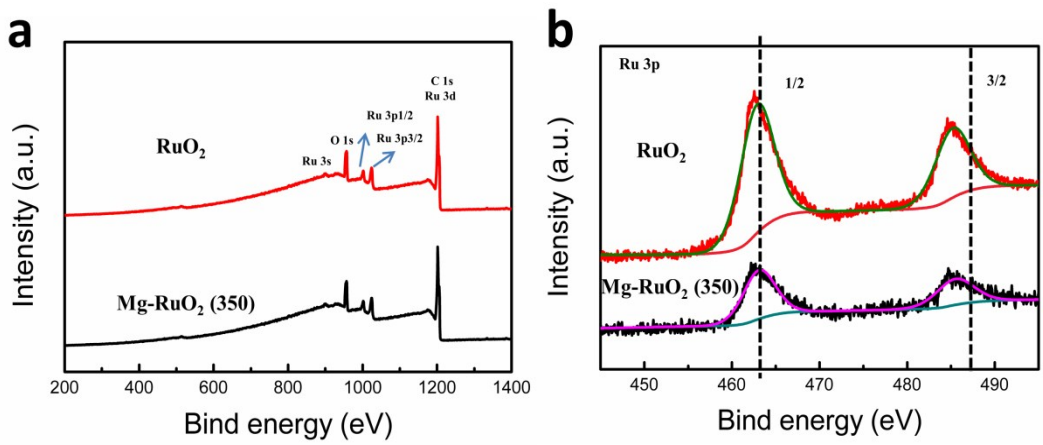

Fig. S7 a) The XPS spectra of Mg-RuO_2 (350) and RuO_2 b) XPS result of Ru 3p spectra enlarged in Figure S4a

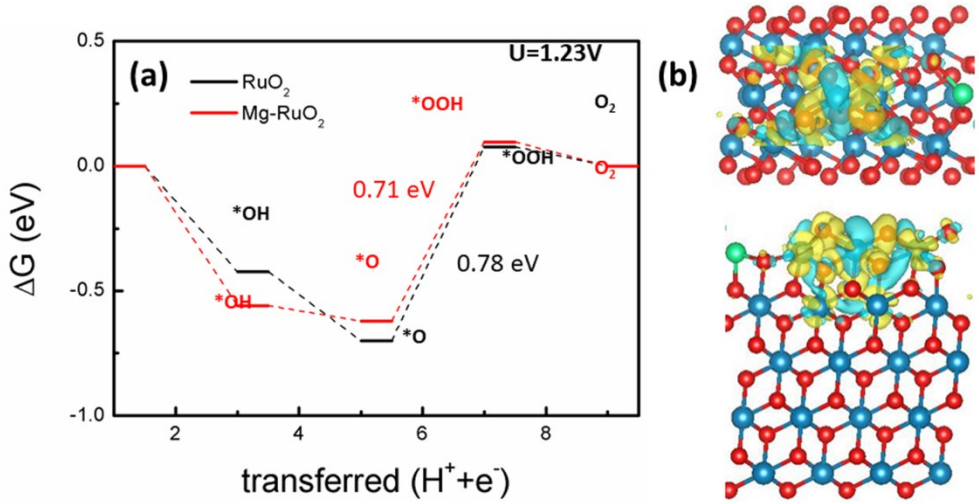

Fig. S8 Comparison of OER free energy profiles of Mg-RuO_2 on (101) and clean RuO_2 (101) in (a); The charge difference distribution on Ru site with Mg dopant is shown in (b)

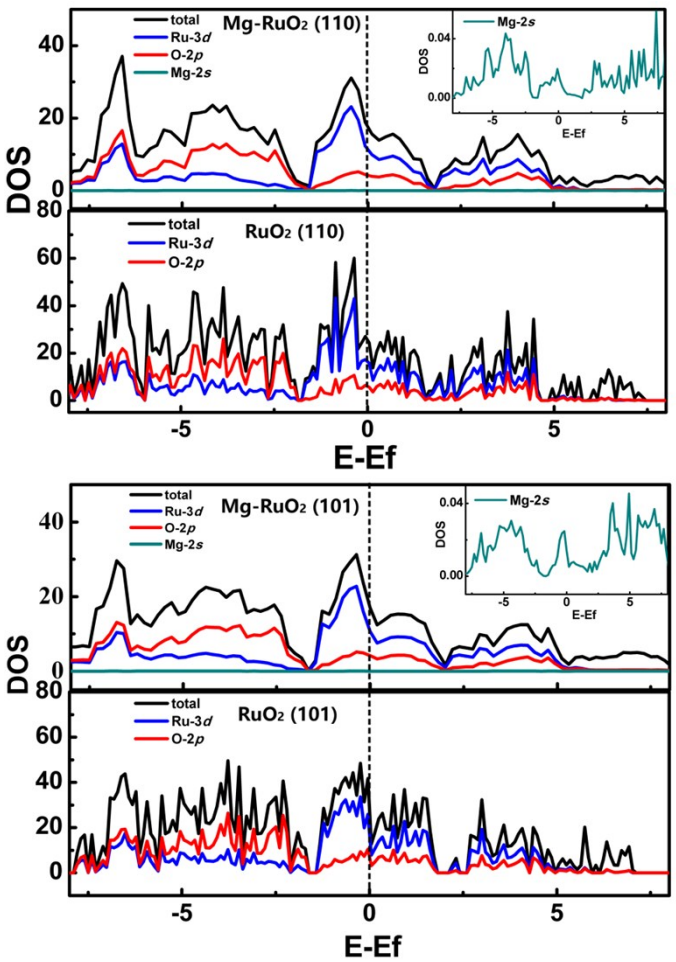

Fig. S9 Comparison of total and local DOS profiles of Mg-doped and clean RuO_2 (101) and (110) to calculate Ru-3*d* band center.

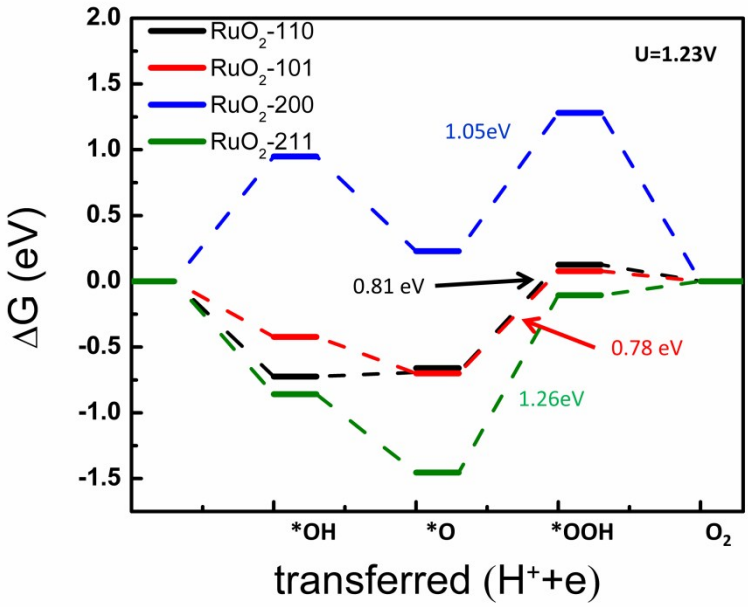

Fig. S10 Comparison of OER free energy profiles of clean RuO_2 on (110), (101), (200) and (211)

References

1. Z. Y. Yao, J. H. Guo, P. Wang, Y. Liu, F. Guo and W. Y. Sun, *Mater. Lett.*, 2018, **223**, 174-177.
2. Z.-Y. Yao, J.-H. Guo, P. Wang, Y. Liu, F. Guo and W.-Y. Sun, *Materials Lett*, 2018, **223**, 174-177.
3. S. Grimme, *J. Comput. Chem. Mater.*, 2006, **27**, 1787-1799.
4. G. Kresse and J. Furthmuller, *Phys. Rev. B*, 1996, **54**, 11169-11186.
5. P. E. Blochl, *Phys. Rev. B*, 1994, **50**, 17953-17979.
6. J. P. Perdew and Y. Wang, *Phys. Rev. B*, 1992, **46**, 12947-12954.
7. S. Grimme, *J. Comput. Chem.*, 2004, **25**, 1463-1473.
8. S. Grimme, S. Ehrlich and L. Goerigk, *J. Comput. Chem.*, 2011, **32**, 1456-1465.
9. J. W. Su, R. X. Ge, K. M. Jiang, Y. Dong, F. Hao, Z. Q. Tian, G. X. Chen and L. Chen, *Adv. Mater.*, 2018, **30**, 1801351.
10. G. Q. Li, S. T. Li, J. J. Ge, C. P. Liu and W. Xing, *J. Mater. Chem. A*, 2017, **5**, 17221-17229.
11. Z. Fan, J. Jiang, L. Ai, Z. Shao and S. Liu, *ACS Appl. Mater. Interfaces*, 2019, **11**, 47894-47903.
12. Y. Lin, Z. Tian, L. Zhang, J. Ma, Z. Jiang, B. J. Deibert, R. Ge and L. Chen, *Nat. Commun.*, 2019, **10**, 162.
13. Y. Lee, J. Suntivich, K. J. May, E. E. Perry and Y. Shao-Horn, *J. Phys. Chem. Lett.*, 2012, **3**, 399-404.
14. Y. M. Hu, X. Luo, G. Wu, T. L. Chao, Z. J. Li, Y. T. Qu, H. Li, Y. Wu, B. Jiang and X. Hong, *ACS Appl. Mater. Interfaces*, 2019, **11**, 42298-42304.
15. J. Shan, C. Guo, Y. Zhu, S. Chen, L. Song, M. Jaroniec, Y. Zheng and S.-Z. Qiao, *Chem*, 2019, **5**, 445-459.
16. J. Shan, T. Ling, K. Davey, Y. Zheng and S.-Z. Qiao, *Adv. Mater.*, 2019, **31**, 1900510.
17. Q. Feng, Q. Wang, Z. Zhang, Y. Xiong, H. Li, Y. Yao, X.-Z. Yuan, M. C. Williams, M. Gu, H. Chen, H. Li and H. Wang, *Appl. Catal.B.*, 2019, **244**, 494-501.
18. J. Kim, P. C. Shih, Y. Qin, Z. Al-Bardan, C. J. Sun and H. Yang, *Angew. Chem. Int. Ed.*, 2018, **57**, 13877-13881.
19. J. Kim, P.-C. Shih, K.-C. Tsao, Y.-T. Pan, X. Yin, C.-J. Sun and H. Yang, *J. Am. Chem. Soc.*, 2017, **139**, 12076-12083.
20. J. Zhang, G. Wang, Z. Liao, P. Zhang, F. Wang, X. Zhuang, E. Zschech and X. Feng, *Nano Energy*, 2017, **40**, 27-33.
21. L. C. Seitz, C. F. Dickens, K. Nishio, Y. Hikita, J. Montoya, A. Doyle, C. Kirk, A. Vojvodic, H. Y. Hwang, J. K. Norskov and T. F. Jaramillo, *Science*, 2016, **353**, 1011-1014.
22. X. Liang, L. Shi, Y. Liu, H. Chen, R. Si, W. Yan, Q. Zhang, G.-D. Li, L. Yang and X. Zou, *Angew. Chem. Int. Ed.*, 2019, **58**, 7631-7635.
23. M. Zhu, Q. Shao, Y. Qian and X. Huang, *Nano Energy*, 2019, **56**, 330-337.
24. Y. Pi, J. Guo, Q. Shao and X. Huang, *Chem. Mater.*, 2018, **30**, 8571-8578.
25. Y. Pi, Q. Shao, P. Wang, J. Guo and X. Huang, *Adv. Funct. Mater.*, 2017, **27**.
26. S. Kumari, B. P. Ajayi, B. Kumar, J. B. Jasinski, M. K. Sunkara and J. M. Spurgeon, *Energy Environ. Sci.*, 2017, **10**, 2432-2440.
27. N. Hong Nhan, H.-S. Oh, T. Reier, E. Willinger, M.-G. Willinger, V. Petkov, D. Teschner and P. Strasser, *Angew. Chem. Int. Ed.*, 2015, **54**, 2975-2979.